

MALDI-TOF Mass Spectrometric Detection of SARS-CoV-2 Using Cellulose Sulfate Ester Enrichment and Hot Acid Treatment

Dapeng Chen,* Wayne A. Bryden,* Catherine Fenselau, Michael McLoughlin, Caroline R. Haddaway, Alese P. Devin, Emily R. Caton, Shelton S. Bradrick, Joy M. Miller, Erin A. Tacheny, M. Megan Lemmon, and Joseph Bogan



Cite This: <https://doi.org/10.1021/acs.jproteome.2c00238>



Read Online

ACCESS |



Metrics & More



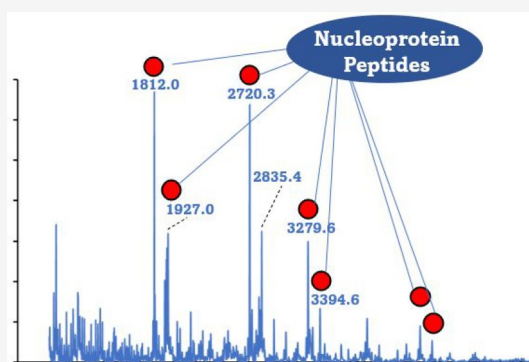
Article Recommendations



Supporting Information

ABSTRACT: Severe acute respiratory syndrome coronavirus 2 (SARS-CoV-2) causes the ongoing coronavirus disease 2019 (COVID-19) pandemic. Here we report a novel strategy for the rapid detection of SARS-CoV-2 based on an enrichment approach exploiting the affinity between the virus and cellulose sulfate ester functional groups, hot acid hydrolysis, and matrix-assisted laser desorption/ionization-time-of-flight mass spectrometry (MALDI-TOF MS). Virus samples were enriched using cellulose sulfate ester microcolumns. Virus peptides were prepared using the hot acid aspartate-selective hydrolysis and characterized by MALDI-TOF MS. Collected spectra were processed with a peptide fingerprint algorithm, and searching parameters were optimized for the detection of SARS-CoV-2. These peptides provide high sequence coverage for nucleocapsid (N protein) and allow confident identification of SARS-CoV-2. Peptide markers contributing to the detection were rigorously identified using bottom-up proteomics. The approach demonstrated in this study holds the potential for developing a rapid assay for COVID-19 diagnosis and detecting virus variants from a variety of sources, such as sewage and nasal swabs.

KEYWORDS: SARS-CoV-2, rapid COVID-19 detection, cellulose sulfate enrichment, hot acid aspartate-selective hydrolysis, MALDI-TOF MS



INTRODUCTION

Matrix-assisted laser desorption/ionization-time-of-flight mass spectrometry (MALDI-TOF MS) and real-time reverse transcription-polymerase chain reaction (RT-PCR) are the well-established molecular technologies in clinical laboratories for detecting causative agents in infectious diseases.^{1,2} RT-PCR is advantageous in its sensitivity and can be directly applied to clinical specimens for detecting pathogens, such as the detection of SARS-CoV-2 for the diagnosis of COVID-19.³ Therefore, RT-PCR has been commonly used as a screening tool in response to community and healthcare-associated infections.⁴ One example is the “MRSA bundle” effort in which RT-PCR is used on nasal swabs to control healthcare-associated infections with methicillin-resistant *Staphylococcus aureus* (MRSA).⁵ The disadvantages of RT-PCR include the costly reagents and lack of multiplexing capacity. Compared to RT-PCR, the main advantages of MALDI-TOF MS include low cost, simplicity, high throughput, and high specificity.⁶ The FDA-approved commercial MALDI-TOF MS platforms currently in use in clinical laboratories globally can identify over 400 species of pathogens from a single colony with an accuracy of >95% in a few minutes.⁷ Because of these

advantages, MALDI-TOF MS has been established as a gold standard in infectious disease diagnosis.

Approaches using MALDI-TOF MS as a diagnostic tool for COVID-19 have been demonstrated.^{8–17} On the basis of the current reports, the detection strategy mainly relies on applying machine learning and artificial intelligence algorithms (AI/ML) to mass peaks (features) extracted from MALDI-TOF MS of either blood, saliva, or nasal swab specimens.^{8–14} Since the mass peaks acquired by MALDI-TOF MS are generated from human specimens, the features that drive the separation between SARS-CoV-2 positive and negative subjects are drawn from both host-response markers and pathogen signatures. As a result, researchers only report masses in MALDI-TOF MS. Neither the origin nor the chemical composition of significant features are known. The approach to detecting COVID-19

Received: April 22, 2022

using SARS-CoV-2 signatures is rare,^{15–17} due to the technical challenges of purifying SARS-CoV-2 from collected samples. Yoshinari et al. made a substantial improvement and reported an approach for the direct detection of SARS-CoV-2 in human nasopharyngeal swabs using a virus purification workflow based on filtration and anion exchange chromatography.¹⁷ In this workflow, nonviral proteins were removed by molecular weight cutoff ultrafiltration (MWCO). The virus was lysed with 2-propanol and the anionic nucleocapsid protein (N protein) was preferentially adsorbed on positively charged Sepharose XL. The enriched N protein was then treated using trypsin digestion, and peptide signatures of the N protein were characterized by MALDI-TOF MS.¹⁷ Yoshinari and coauthors made critical contributions to the unambiguous detection of SARS-CoV-2 using pathogen signatures. However, the virus purification and peptide preparation protocols are labor-intensive and slow, as they include ultra-high-speed centrifugation and trypsin digestion.¹⁷

Compared to bacteria identification, virus identification using MALDI-TOF MS faces critical challenges that hamper its application in clinical laboratories, including the difficulty of acquiring an enriched virus sample and the scarcity of characteristic mass peaks related to characteristic viral proteomes.^{18–22} Molecular docking studies showed that spike proteins of SARS-CoV-2 interact with cellular heparin sulfate and angiotensin-converting enzyme 2 (ACE2) to initiate cellular entrance.^{23,24} It was also shown that heparin binds spike proteins *in vitro*, suggesting that cellulose sulfate functional groups can be used to enrich SARS-CoV-2.²⁴ In this study we hypothesized that cellulose sulfate ester columns could be used as an enrichment method for SARS-CoV-2, and a rapid detection approach can be developed on the basis of peptide profiles from the enriched sample provided by MALDI-TOF MS.

MATERIALS AND METHODS

Materials

Sulfate ester-immobilized on cellulose beads (Cellufine Sulfate) were commercially acquired from JNC Corporation (Tokyo, Japan). Phosphate-buffered saline (PBS, pH 7.4) solutions, glacial acetic acid, HPLC water, and acetonitrile were purchased from Thermo Fisher Scientific (Waltham, MA). Alpha-cyano-4-hydroxycinnamic acid (CHCA) MALDI-TOF MS matrix was purchased from MilliporeSigma (St. Louis, MO).

Viral Sample Preparation

Vero E6 cells expressing human TMPRSS2 (Vero E6-TMPRSS2) were obtained from the Japanese Collection of Research Bioresources and maintained in Gibco DMEM/F12 media (Thermo Fisher Scientific) supplemented with 10% fetal bovine serum (VWR, Radnor, PA), penicillin (100 unit/mL)/streptomycin (100 µg/mL; VWR), and 1 mg/mL Gibco Geneticin (Thermo Fisher Scientific). SARS-CoV-2 (hCoV-19/Japan/TY7-503/2021) was obtained from BEI Resources and propagated in Vero E6-TMPRSS2. Briefly, 3×10^7 cells were plated into a T-175 flask and infected 24 h later at a cell density of ~90%. Cells were infected with a dose of 7.1×10^7 TCID₅₀ (50% tissue culture infectious dose) in 5 mL of Dulbecco's PBS (DPBS; Thermo Fisher Scientific) for 1 h at 37 °C. After absorption, 15 mL of DMEM/F12 with 2% FBS was added, and cells were further incubated at 37 °C, 5% CO₂ for 48 h, at which point 90% cytopathic effect was observed.

Virus-containing media was harvested, aliquoted, and stored at –80 °C. All work with live virus was conducted in a Biosafety Level-3 (BSL-3) laboratory with adherence to established safety guidelines.

For virus analysis, 2 mL of virus stock was thawed and subjected to centrifugation at 1000g for 10 min to clarify cell debris. The virus was then layered onto a 34% w/v sucrose cushion in DPBS and pelleted in an ultracentrifuge for 1 h at 100 000g and 4 °C. After centrifugation, the supernatant was discarded, and the virus pellet was resuspended in 2 mL of pure water. Prior to analysis, virus infectivity was inactivated by incubation at 70 °C for 30 min. Inactivation was confirmed by plating 10% of the material on naïve Vero E6 TMPRSS2 cells and monitoring the cytopathic effect (CPE) at 6 days postinfection. The virus titer in the final sample after concentration is 2.3×10^7 TCID₅₀/mL or plaque-forming units/mL (PFU/mL).

Construction of the Cellulose Sulfate Ester Columns

For packing the columns, 200 mg of cellulose sulfate ester beads were packed into a microcolumn following the method previously described.²⁵ Generally, a frit disk was installed on the bottom of the microcolumn, and 200 mg of beads were loaded. Another frit disk was installed on top of the beads. The packed column can be stored at room temperature before use. The packed columns were washed with 500 µL of 10×PBS once and 500 µL of 1×PBS three times for further use.

Cellulose Sulfate Ester Column Enrichment of SARS-CoV-2

The workflow is shown in Figure 1. For the enrichment, 450 µL of virus sample was prepared in 10×PBS to make a final

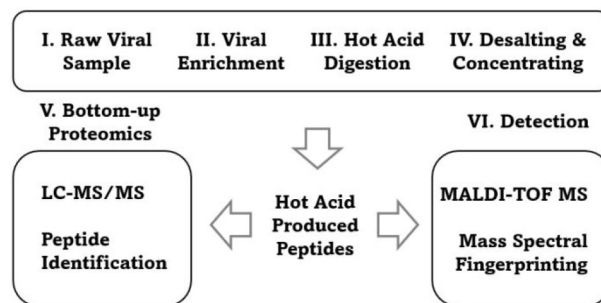


Figure 1. Overview of workflow for the identification of viral peptides using bottom-up proteomics and the rapid detection of SARS-CoV-2 using MALDI-TOF MS and peptide fingerprinting. Experiment duration from sample to result in the rapid MALDI-TOF MS workflow (29 min): viral enrichment (5 min), hot acid digestion (15 min), peptide desalting concentration (3 min), MALDI-TOF MS sample preparation (3 min), MALDI-TOF MS data acquisition (2 min), mass spectral fingerprinting (1 min).

solution of 1×PBS solution. The virus sample solution was loaded into the column using a syringe and pushed through very slowly. The flow-through sample was collected and pushed through the column five more times, making six times total. To completely remove nonbinding proteins, 2 mL of 0.2 M NaCl in 1×PBS washing solution was pushed through the column three times very slowly. 900 µL of 1.5 M NaCl in 1×PBS elution solution was pushed through the column rapidly using the syringe, and the elution sample was collected. The sample loading and washing took 5 min. To remove 10×PBS from the virus solution, the sample was loaded into a 3K cutoff filter column and spun in a microcentrifuge at

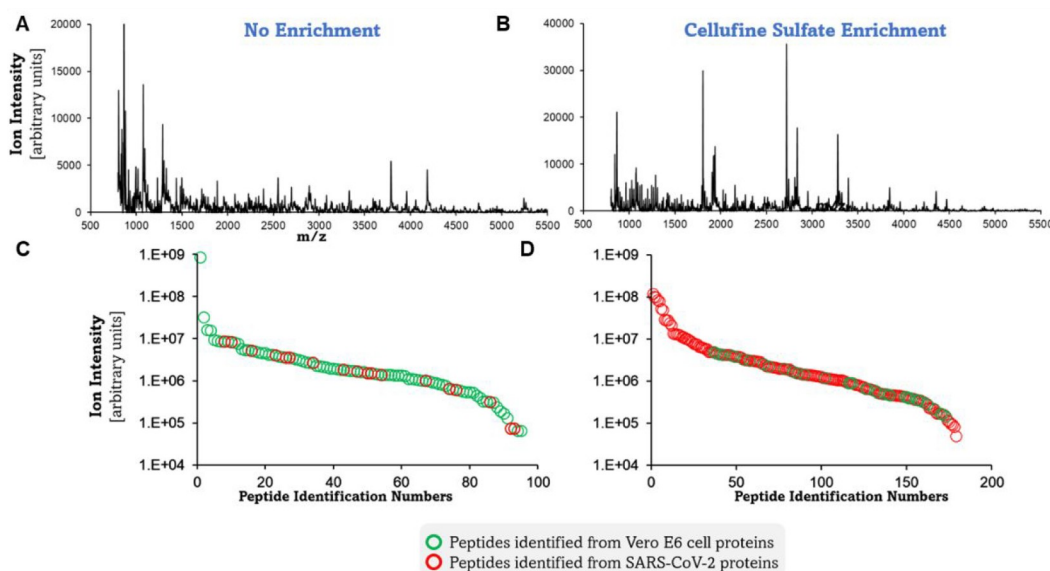


Figure 2. Characterization of peptides produced from hot acid treatment before and after cellulose sulfate column enrichment using MALDI-TOF MS and bottom-up proteomics. (A) MALDI-TOF mass spectrum of peptides from a raw sample. (B) MALDI-TOF mass spectrum of peptides produced following enrichment. (C) Distribution of peptide ion intensities measured in the raw sample using bottom-up proteomics. (D) Distribution of peptide ion intensities measured in the enriched sample using bottom-up proteomics. Green circles indicate peptides assigned to Vero E6 cell proteins and red circles indicate peptides assigned to SARS-CoV-2 proteins.

14 000g for 25 min. Alternatively, the removal of PBS can be done by using C18 tips reported in our previous studies, which is more rapid and inexpensive.^{26,27} After desalting, the sample can be directly applied to the following experimental procedure.

Hot Acid Digestion

The sample produced from the 3K cutoff filtration was moved to a snap cap thin-wall PCR microtube and topped with HPLC water to make a final sample volume of 87.5 μ L. 12.5 μ L of glacial acetic acid was added to make a 12.5% acid solution. The solution was incubated on a heating block at 140 $^{\circ}$ C for 15 min. After incubation, the microtube was immediately cooled using cold water to stop the protein hydrolysis. The hot acid digestion conditions were optimized using a protein standard Bovine Serum Albumin Standard Ampules (Thermo Scientific, Figure S1).

MALDI-TOF Mass Spectrometry

CHCA MALDI matrix (9 mg/mL) was prepared in 70% acetonitrile. For MALDI-TOF MS, 1.0 μ L of the hot acid sample was deposited onto the MALDI plate and dried. Then, 1.0 μ L of the CHCA solution was deposited on top and mixed by pipetting up and down. The samples were evaluated on a Bruker Daltonics microflex LRF MALDI-TOF mass spectrometer (Billerica MA). MALDI-TOF mass spectra were obtained in the positive linear mode, and an average of 600 profiles were collected in a mass range of 700–21 000 m/z . The MALDI-TOF MS preparation and data collection took 5 min. All experiments were repeated three times to ensure repeatability.

Bottom-up Proteomics

Peptides after hot acid treatment were desalted and concentrated using C18 Tiptip (Glygen Corp., Columbia, MD) for bottom-up proteomics. The peptides were resuspended in 50 μ L of HPLC water before being injected into an EASY-nLC 1000 system (Thermo Fisher Scientific)

coupled with an LTQ Orbitrap system (Thermo Fisher Scientific). An Acclaim PepMap 100 C18 trap column (0.2 mm \times 20 mm, 5 μ L/min) and an analytical column (75 μ m \times 150 mm, 300 nL/min) were used, and peptides were separated using 80% ACN prepared in 0.1% FA in 60 min. For protein identification, raw data files were loaded into MaxQuant (maxquant.org) and searched against a protein database (UniProtKB/Swiss-Prot, UniProt.org) containing reviewed proteins of SARS-CoV-2 and Vero E6 cell line (African green monkey, *Cercopithecus aethiops*). Oxidation (M) was selected for variable modification. Digestion was set to the C terminus and N terminus of aspartic acid (D). Four missed cleavage sites were allowed. False discovery rates (FDR) for both peptide and protein identification were 0.01. We used the default values for other parameters in MaxQuant.

Protein Identification and Detection of SARS-CoV-2 Using Peptide Fingerprinting

The online program MASCOT Peptide Mass Fingerprint (Matrix Science, Boston, MA, matrixscience.com) was used with MALDI-TOF MS data. Mass peaks with S/N > 10 in MALDI-TOF MS were extracted into “Mass values” for analysis. “SwissProt” protein database was used, and “All entries” was selected for taxonomy. Enzyme was defined as “Formic acid,” and different missed cleavage numbers, 0–9, were allowed. Peptide tolerance was set to 0.5 Da, and monoisotopic type was selected. The protein identification by peptide fingerprinting took less than a minute to complete. The definitions of the parameters are available at the online “Tutorial” program under “Peptide Mass Fingerprint search” (matrixscience.com).

RESULTS AND DISCUSSION

Proteomic Analysis of SARS-CoV-2 Enriched Using Cellulose Sulfate Ester Columns

The virus samples were prepared in Vero E6 cells. Proteins identified in the raw virus sample (unenriched virus sample)

Table 1. Identification of NCAP_SARS2 (N Protein) Using the Peptide Mass Fingerprint Program from MALDI-TOF MS^a

allowed missed cleavage	score	expect	matches
0	59	0.78	6
1	126	1.40×10^{-07}	15
2	211	4.50×10^{-16}	24
3	250	5.70×10^{-20}	28
4	230	5.70×10^{-18}	28
5	236	1.40×10^{-18}	29
6	232	3.60×10^{-18}	29
7	231	4.50×10^{-18}	29
8	230	5.70×10^{-18}	29
9	230	5.70×10^{-18}	29

^aA score greater than 70 is significant ($p < 0.05$) for protein identification (matrixscience.com). "Expect" means expectation values (E-value). "Matches" means the matched input mass values in MALDI-TOF MS to calculated mass values generated from the defined protein digestion.

UniProtKB - P0DTC9 (NCAP_SARS2)	
1	MSDNGPQNR NAPRITFGGP SDSTGSNQNG ERSGARSKQR RPQGLPNNTA
51	SWFTALTQHG KEDLKFPRGQ GVPINTNSSP DDQIGYYRRA TRRIRGGDGK
101	MKDLSPRWYF YYLGTGPEAG LPYGANKDGI IWVATEGALN TPKDHIGTRN
151	PANNAIVLQ LPQGTTLPGK FYAEGSRGGS QASSRSSRS RNSSRNSTPG
201	SSRGTSPARM AGNGGDAALA LLLDLRLNQL ESKMSGKQQ QQGQVTKKS
251	AAEASKKPRQ KRTATKAYNV TQAFGRGPE QTQGNFGDQE LIRQGTDYKH
301	WPQIAQFAPS ASAFFGMSRI GMEVTPSGTW LTYTGAIKLD DKDPNFKDQV
351	ILLNKHIDAY KTFPTEPKK DKKKKADETQ ALPQRQKKQQ TVTLLPAADL
401	DDFSKQLQSS MSSADSTQA

Figure 3. NCAP_SARS2 (N protein) sequence coverage. Red residues are present in peptides identified.

using peptide identification with bottom-up proteomics showed that host cell proteins were the most readily identified proteins, including DNA deaminase, hepatitis A virus cellular receptor 1, and calreticulin (Table S1, Table S2). Viral protein ORF3c was also identified on the basis of peptides in the raw virus samples (Table S1). The difference in peptide ion intensities between host cells and virus is around 100 times (Figure 2, Table S1, Table S2). After virus enrichment on the cellulose sulfate ester column, peptides of the N protein of SARS-CoV-2 were the most abundant peptides detected (Table S3, Table S4, Figure 2). Peptide fingerprints revealed by MALDI-TOF MS showed different patterns between the raw virus sample and the virus sample enriched on the cellulose sulfate ester column (Figure 2A,B). The mass shift signature characteristic of hot acid protein hydrolysis, +115.1 Da of adding or removing an aspartic acid residue, was observed for the peak assignments (Table S4). These are identified as missed cleavages in the software used (Table S4).

The improvement in the identification of viral peptides with the enrichment is also revealed by the ion intensity values (Figure 2C,D). The ion intensity of the peptides was 1.2×10^8 , while no peptides of the host cell proteins were identified above the ion intensity of 6.5×10^6 (Figure 2D). The peptide analysis using bottom-up proteomics indicates that cellulose sulfate ester provides a significant enrichment of SARS-CoV-2, based on the affinity between the cellulose sulfate ester functional groups and SARS-CoV-2. The enrichment experiments were repeated in this study to show the reproducibility (Figure S2, S3).

Bottom-up proteomics identified abundant peptides belonging to the N protein with cellulose sulfate ester column enrichment (Table S3). It is well reported that spike proteins of the SARS-CoV-2 viral wall show affinity to cellulose sulfate functional groups via glycan-binding domains.²³ However, spike proteins were not identified in the enrichment samples using bottom-up proteomics. We hypothesize that this is mainly caused by the relative abundances of viral proteins in the virus and heavy post-translational modification of spike proteins. Bottom-up proteomics in this study showed that the N protein was the most abundant based on the ion intensity in the orbitrap mass spectrometer, which agrees well with previous studies in which viral protein profiles were revealed by mass spectrometry.^{28–32} Gouveia and Saadi showed that the ion intensities of two peptides of the N protein were the most intense in nanoLC-MS/MS using COVID-19 clinical samples.^{28,32} Nikolaev and coauthors concluded that the N protein was the best candidate for mass spectrometric detection due to the N protein's high abundance and the presence in the lowest viral loads of patient samples.²⁹ Ihling and coauthors reported that the N protein is the only identified one in highly diluted gargle solutions of COVID-19 patients.³⁰ Bezstarosti and coauthors identified several viral proteins using targeted mass spectrometry in virus samples prepared from Vero E6 cells and found that the N protein was the most abundant one, followed by the spike protein.³¹ It was shown that the ion intensity of the N protein was ~20 times higher than spike proteins.³¹ The MALDI-TOF MS in our study is consistent with the previous reports, as peptides of the N protein are the most intense mass peaks. SARS-CoV-2 proteome database (UniProt.org) shows that the spike protein is heavily modified by post-translational modifications, including 14 cysteine disulfide bonds, 10 amino acid lipidations, and over 20 glycosylation sites. On the other hand, heavy post-translational modifications have not been reported on the N protein. Due to the heavy modifications, peptides of the spike proteins generated from hot acid treatment may not be feasibly identified in the database searching algorithm. In addition, it is still unknown how many post-translational modifications affect hot acid protein hydrolysis. The large size glycans may prevent aspartic acid sites from being cleaved.

Since growth media and host cells are used for virus propagation, contaminant proteins, such as bovine serum albumin, are the dominant materials in raw viral samples.¹⁶ Antibody-based affinity, ultrahigh-speed centrifugation, and ultrafiltration methods have been proposed to enrich viral materials.¹⁷ The sulfate ester column-based enrichment method we present in this study has several advantages. Compared with other enrichment methods, our column-based method only requires sample loading, washing, and elution, which can be done feasibly without intensive personnel training. In addition, the sulfate ester columns and solutions are inexpensive, autoclavable, and can be stored at room temperature for a long time. For example, the commercial cellulose sulfate ester beads used in this study can be stored at room temperature for three years.

Clinical pathogen identification using MALDI-TOF MS relies on mass spectral fingerprints generated from house-keeping proteins such as ribosome proteins in bacteria.¹⁷ Compared to bacterium identification, virus identification is mainly limited by viruses' simple proteome. For example, the MALDI-TOF spectrum of bacteriophage MS2 only contains one mass, that of the intact capsid protein.¹⁸ SARS-CoV-2

Table 2. Peptides Identified from the Nucleocapsid Protein Using 3 Allowed Missed Cleavages Using MASCOT Peptide Mass Fingerprint Program^a

matched peptide	sequence (AA)		observed	Mr(expt)
	start	end	MH+	M
M.SDNGPQNQRNAPRITFGGPS.D	2	22	2228.0	2227.037
D.NGPQNQRNAPRITFGGPS.D	4	21	1911.0	1909.951
D.STGSNQNGERSGARSKQRRPQGLPNNTASWFTALTQHGKED.L	23	63	4469.2	4468.173
D.LKFPRGQGVPIINTNSP.D	64	80	1812.0	1810.969
D.LKFPRGQGVPIINTNSPD.D	64	81	1927.0	1925.996
D.LKFPRGQGVPIINTNSPDD.Q	64	82	2042.0	2041.023
D.QJGYRRATRRIRGGD.G	83	98	1938.0	1937.046
D.GKMKDLSRWYFYLLGTGPEAGLPYGANK.D	99	127	3279.6	3278.622
D.GKMKDLSRWYFYLLGTGPEAGLPYGANKD.G	99	128	3394.6	3393.649
D.LSPRWYFYLLGTGPEAGLPYGANK.D	104	127	2720.3	2719.343
D.LSPRWYFYLLGTGPEAGLPYGANKD.G	104	128	2835.4	2834.37
K.DGIWVATEGALNTPK.D	128	144	1799.8	1798.91
D.GIIWVATEGALNTPK.D	129	143	1569.9	1568.856
D.GIIWVATEGALNTPK.D.H	129	144	1684.9	1683.883
G.DQELIRQGT.D.Y	288	297	1174.6	1173.563
D.QELIRQGT.D.Y	289	297	1059.5	1058.536
D.PNFKDQVILLNK.H.I.D	344	357	1679.0	1677.957
D.AYKTFPPTEPKK.D	359	370	1406.8	1405.761
D.AYKTFPPTEPKK.D.K	359	371	1521.8	1520.788
D.AYKTFPPTEPKKDKKKAD.E	359	377	2220.2	2219.231
D.KKKKADETQALPQRQKKQQTVTLLPAA.D	372	398	3047.8	3046.761
A.DETQALPQRQKKQQTVTLLPAA.D	377	399	2579.4	2578.371
D.ETQALPQRQKKQQTVTLLPAA.D	378	398	2349.3	2348.318
D.ETQALPQRQKKQQTVTLLPAA.DLD.D	378	401	2692.5	2691.456
D.LDDFSKQLQQSMSSA.D	400	414	1684.8	1683.777
D.DFSKQLQQSMSSAD.S	402	415	1571.7	1570.693
D.FSKQLQQSMSSAD.S	403	415	1456.7	1455.666
D.FSKQLQQSMSSADSTQA.-	403	419	1843.8	1842.842

^a“Observed” means the mass values measured in MALDI-TOF MS. “Mr(expt)” means the theoretical molecular mass of the matched peptide.

proteome contains more proteins than bacteriophage MS2, but the molecular weights of those proteins exceed the optimized mass range of MALDI-TOF MS. Approaches focusing on characterizing the digestion products of viral proteins have been developed to overcome these limitations.^{17,18,20,21,32}

Trypsin has been used as a gold standard for protein digestion for proteomics, mainly due to its high specificity. However, the tryptic reaction is slow and requires a well-controlled reaction temperature and pH solution to avoid autolysis. Because of these limitations, a hot acid-based protein hydrolysis method was developed to provide peptides for virus identification.^{18,20,21} Advantages of using the hot acid approach include the use of a stable inexpensive organic acid and a rapid digestion process. Compared to trypsin digestion, peptide signatures can be observed in as short as 30 s into the hot acid reaction without protein reduction, and alkylation that is usually required for trypsin digestion.¹⁸

Rapid Detection of SARS-CoV-2 Using MALDI-TOF MS and Peptide Mass Fingerprinting

Since most of the peptides identified after enrichment belong to the N protein of the SARS-CoV-2 virus, we hypothesized that the mass peaks detected by MALDI-TOF MS after enrichment could constitute a marker suite to be used for the identification of this virus based on a peptide fingerprinting algorithm. For this purpose, we examined the 37 mass peaks in the MALDI spectrum with signal-to-noise ratios larger than 10 with the MASCOT Peptide Mass Fingerprint program

(matrixscience.com) (Table S5). Hot acid protein hydrolysis occurs on both sides of aspartate, and the MASCOT program classifies some products as carrying missed cleavages.^{26,27} We evaluated the effect of missed cleavages on the identification scores. The results show that the N protein is more confidently identified when missed cleavages are allowed (Table 1). Among the identification results, 3 allowed missed cleavage sites resulted in the best score, and the score did not vary significantly when larger missed cleavage numbers were used (Table 1).

The peptide list extracted by MASCOT Peptide Mass Fingerprint shows that 54% of the sequence of the N protein was identified and suggests the high efficiency of the hot acid treatment method (Figure 3, Table 2). The unidentified central portion of the protein contains two aspartate residues, and small peptides are not produced (Figure 3).

The dominance of mass peaks assigned to the N protein in MALDI-TOF MS provides superior advantages for the rapid detection of SARS-CoV-2 using the peptide fingerprinting algorithm. In the raw virus sample, mass peaks assigned to peptides of Vero E6 cell proteins are dominant in MALDI-TOF MS. However, since these peptides are produced from different proteins, the peptide fingerprint algorithm fails to identify those proteins (Table S6).

This study demonstrates a rapid SARS-CoV-2 detection strategy based on cellulose sulfate ester enrichment, hot acid protein hydrolysis, and peptide fingerprinting with MALDI-TOF MS. The materials and solvents used in this approach are

inexpensive, and the whole detection process can take less than 30 min (Figure 1). Although cellular entrance mechanisms by toxins and viruses have been explored extensively for enrichment purposes,^{33–36} we demonstrate for the first time that the interaction between cellulose sulfate functional groups and SARS-CoV-2 can be used for the enrichment. The interaction happens via glycan sites on spike proteins based on the reported mechanisms.^{23,24} Our method exploits cellulose sulfate ester binding by using a minimal synthetic substrate immobilized in a microcolumn and has the potential for automation for clinical use. Yoshinari et al. reported that the titers of SARS-CoV-2 copy numbers in clinical nasopharyngeal swabs were estimated between $10^{3.9}$ and $10^{6.3}$ PFU per mL.¹⁷ The estimated titer for the confident identification of SARS-CoV-2 based on the fingerprinting reported in our study is $10^{5.1}$ PFU per mL, suggesting our approach can detect SARS-CoV-2 in various clinical specimens.

Another potential use is the integration of our approach with the current wastewater surveillance efforts to measure SARS-CoV-2 to track community infection dynamics (cdc.gov).³⁷ The current surveillance technology relies on the detection of viral RNA using PCR. It was reported that the primary sludge contained between 1.7×10^3 to 4.6×10^5 mL⁻¹ SARS-CoV-2 viral RNA copies measured by quantitative reverse transcription polymerase chain reaction (qRT-PCR).³⁷ Our approach presented in this study can be used as an inexpensive and rapid alternative to the current SARS-CoV-2 surveillance technology.

On the basis of the peptide profiles of the N protein, our approach has the potential to identify virus variants. Omicron/B.1.1.529 has a P → L transition at amino acid position 13 (UniProt.org), and the change in sequence and mass occurs within peptides that are detected in our sample. For example, SDNGPQNQRNAP(L)RITFGGPSD will have a mass shift from 2228.0 to 2244.1 *m/z* (Table 2). However, the mutation from an aspartate residue to another residue in other variants may reduce the coverage. For example, Delta/B.1.617.2 has a D → Y transition at amino acid position 377 (UniProt.org), and D(Y)ETQALPQRQKKQQTVTLLPAAD will not be cleaved by the hot acid (Table 2), resulting in a larger peptide.

It should be noted that the interaction between SARS-CoV-2 and cellulose sulfate functional groups is not unique. Other studies reported the use of cellulose sulfate columns to enrich other virus types, such as influenza.^{38–41} The coinfection of influenza and SARS-CoV-2 is rare but has been reported.⁴² For coinfection cases, a more sophisticated identification algorithm is needed for multiplexing. Other glycoproteins contained in clinical specimens may also be captured by cellulose sulfate and contribute to the MALDI spectrum.

CONCLUSION

In this study, we have demonstrated a strategy using cellulose sulfate ester enrichment and hot acid protein hydrolysis for the rapid mass spectrometric detection of SARS-CoV-2. Our strategy has adequate sensitivity and specificity, based on high sequence coverage for the signature nucleocapsid protein of SARS-CoV-2. Due to its simplicity and robustness, our approach has the potential for automation. This strategy can be extended to other virus types that show affinity to cellulose sulfate functional groups.

ASSOCIATED CONTENT

Supporting Information

The Supporting Information is available free of charge at <https://pubs.acs.org/doi/10.1021/acs.jproteome.2c00238>.

Figure S1: MALDI-TOF mass spectra of repeated measurements of digested BSA standard protein; Figure S2: MALDI-TOF mass spectra of repeated measurements of digested virus samples with the enrichment; Figure S3: MALDI-TOF mass spectra of repeated measurements of digested virus samples without the enrichment; Table S1: Protein groups identified from the raw virus sample using bottom-up proteomics; Table S2: Peptides identified from the raw virus sample using bottom-up proteomics; Table S3: Protein groups identified from the enriched virus sample using bottom-up proteomics; Table S4: Peptides identified from the enriched virus sample using bottom-up proteomics; Table S5: MASCOT peptide fingerprinting results in the enriched virus sample; Table S6: MASCOT peptide fingerprinting results in the raw virus sample (PDF)

AUTHOR INFORMATION

Corresponding Authors

Dapeng Chen – Zeteo Tech, Inc., Sykesville, Maryland 21784, United States; orcid.org/0000-0001-8412-581X; Email: dapeng.chen@zeteotech.com

Wayne A. Bryden – Zeteo Tech, Inc., Sykesville, Maryland 21784, United States; Email: wayne.bryden@zeteotech.com

Authors

Catherine Fenselau – Department of Chemistry and Biochemistry, University of Maryland, College Park, Maryland 20742, United States; orcid.org/0000-0003-4979-0229

Michael McLoughlin – Zeteo Tech, Inc., Sykesville, Maryland 21784, United States

Caroline R. Haddaway – Zeteo Tech, Inc., Sykesville, Maryland 21784, United States

Alese P. Devin – Zeteo Tech, Inc., Sykesville, Maryland 21784, United States

Emily R. Caton – Zeteo Tech, Inc., Sykesville, Maryland 21784, United States

Shelton S. Bradrick – MRIGlobal, Kansas City, Missouri 64110, United States

Joy M. Miller – MRIGlobal, Kansas City, Missouri 64110, United States

Erin A. Tacheny – MRIGlobal, Gaithersburg, Maryland 20878, United States

M. Megan Lemmon – MRIGlobal, Gaithersburg, Maryland 20878, United States

Joseph Bogan – MRIGlobal, Gaithersburg, Maryland 20878, United States

Complete contact information is available at:

<https://pubs.acs.org/doi/10.1021/acs.jproteome.2c00238>

Author Contributions

Conceptualization: D.C., W.A.B., and C.F. Experiment design: D.C., W.A.B., and M.M. Virus sample preparation: S.S.B. and J.M.M. Virus experiments: C.R.H., A.P.D., E.R.C., E.A.T.,

M.M.L., and J.B. MALDI-TOF MS: C.R.H. and A.P.D. Bottom-up proteomics: D.C. Manuscript drafting: D.C. and C.R.H. All authors understood the results. All authors approved the manuscript.

Funding

All the work in the study was supported by Zeteo Tech's internal research and development fund.

Notes

The authors declare the following competing financial interest(s): W.A.B., M.M., D.C., A.P.D., E.R.C., and C.R.H. have competing financial interests. W.A.B. is the President and CEO of Zeteo Tech, Inc. M.M. is the Vice President of Zeteo Tech, Inc. D.C., A.P.D., E.R.C., and C.R.H. are employed by Zeteo Tech, Inc. An unpublished U.S. Provisional Patent Application assigned to Zeteo Tech, Inc. was applied based on this research. C.F., S.S.B., J.M.M., E.A.T., M.M.L., and J.B. declare no competing interests.

Data Repository: <https://chorusproject.org/pages/authentication.html>. Project ID 1774.

REFERENCES

- (1) Fenselau, C.; Demirev, P. A. Characterization of intact microorganisms by MALDI mass spectrometry. *Mass Spectrom. Rev.* **2001**, *20*, 157–171.
- (2) Espy, M. J.; Uhl, J. R.; Sloan, L. M.; Buckwalter, S. P.; Jones, M. F.; Vetter, E. A.; Yao, J. D. C.; Wengenack, N. L.; Rosenblatt, J. E.; Cockerill, F. R., III; Smith, T. Real-time PCR in clinical microbiology: applications for routine laboratory testing. *Clin. Microbiol. Rev.* **2006**, *19*, 165–256.
- (3) Long, C.; Xu, H.; Shen, Q.; Zhang, X.; Fan, B.; Wang, C.; Zeng, B.; Li, Z.; Li, X.; Li, H. Diagnosis of the Coronavirus disease (COVID-19): rRT-PCR or CT? *European journal of radiology* **2020**, *126*, 108961.
- (4) Wang, R.; Taubenberger, J. K. 2010. Methods for molecular surveillance of influenza. *Expert review of anti-infective therapy* **2010**, *8*, S17–S27.
- (5) Jain, R.; Kralovic, S. M.; Evans, M. E.; Ambrose, M.; Simbartl, L. A.; Obrosky, D. S.; Render, M. L.; Freyberg, R. W.; Jernigan, J. A.; Muder, R. R.; Miller, L. J.; Roselle, G. A. Veterans Affairs initiative to prevent methicillin-resistant *Staphylococcus aureus* infections. *N. Engl. J. Med.* **2011**, *364*, 1419–1430.
- (6) Carbonnelle, E.; Beretti, J. L.; Cottyn, S.; Quesne, G.; Berche, P.; Nassif, X.; Ferroni, A. 2007. Rapid identification of *Staphylococci* isolated in clinical microbiology laboratories by matrix-assisted laser desorption ionization-time of flight mass spectrometry. *Journal of clinical microbiology* **2007**, *45*, 2156–2161.
- (7) Lévesque, S.; Dufresne, P. J.; Soualhine, H.; Domingo, M. C.; Bekal, S.; Lefebvre, B.; Tremblay, C. 2015. A side by side comparison of Bruker Biotyper and VITEK MS: utility of MALDI-TOF MS technology for microorganism identification in a public health reference laboratory. *PLoS one* **2015**, *10*, e0144878.
- (8) Tran, N. K.; Howard, T.; Walsh, R.; Pepper, J.; Loegering, J.; Phinney, B.; Salemi, M. R.; Rashidi, H. H. Novel application of automated machine learning with MALDI-TOF-MS for rapid high-throughput screening of COVID-19: A proof of concept. *Sci. Rep.* **2021**, *11*, 1–10.
- (9) Yan, L.; Yi, J.; Huang, C.; Zhang, J.; Fu, S.; Li, Z.; Lyu, Q.; Xu, Y.; Wang, K.; Yang, H.; Ma, Q.; Cui, X.; Qiao, L.; Sun, W.; Liao, P. Rapid detection of COVID-19 using MALDI-TOF-based serum peptidome profiling. *Anal. Chem.* **2021**, *93*, 4782–4787.
- (10) Rocca, M. F.; Zintgraff, J. C.; Dattero, M. E.; Santos, L. S.; Ledesma, M.; Vay, C.; Prieto, M.; Benedetti, E.; Avaro, M.; Russo, M.; Nachtigall, F. M.; Baumeister, E. A combined approach of MALDI-TOF mass spectrometry and multivariate analysis as a potential tool for the detection of SARS-CoV-2 virus in nasopharyngeal swabs. *J. Virol. Methods* **2020**, *286*, 113991.
- (11) Lazari, L. C.; Zerbinati, R. M.; Rosa-Fernandes, L.; Santiago, V. F.; Rosa, K. F.; Angeli, C. B.; Schwab, G.; Palmieri, M.; Sarmiento, D. J. S.; Marinho, C. R. F.; Almeida, J. D.; To, K.; Giannecchini, S.; Wrenger, C.; Sabino, E. C.; Martinho, H.; Lindoso, J. A. L.; Durigon, E. L.; Braz-Silva, P. H.; Palmisano, G. MALDI-TOF mass spectrometry of saliva samples as a prognostic tool for COVID-19. *J. Oral Microbiol.* **2022**, *14*, 2043651.
- (12) Deulofeu, M.; García-Cuesta, E.; Peña-Méndez, E. M.; Conde, J. E.; Jiménez-Romero, O.; Verdú, E.; Serrano, M. T.; Salvadó, V.; Boadas-Vaello, P. Detection of SARS-CoV-2 infection in human nasopharyngeal samples by combining MALDI-TOF MS and artificial intelligence. *Front. Med.* **2021**, *8*, 398.
- (13) Costa, M. M.; Martin, H.; Estellon, B.; Dupé, F. X.; Saby, F.; Benoit, N.; Tissot-Dupont, H.; Million, M.; Pradines, B.; Granjeaud, S.; Almeras, L. Exploratory study on application of MALDI-TOF-MS to detect SARS-CoV-2 infection in human saliva. *Journal of Clinical Medicine* **2022**, *11*, 295.
- (14) Nachtigall, F. M.; Pereira, A.; Trofymchuk, O. S.; Santos, L. S. Detection of SARS-CoV-2 in nasal swabs using MALDI-MS. *Nature biotechnology* **2020**, *38*, 1168–1173.
- (15) Chivte, P.; LaCasse, Z.; Seethi, V. D. R.; Bharti, P.; Bland, J.; Kadkol, S. S.; Gaillard, E. R. MALDI-ToF protein profiling as a potential rapid diagnostic platform for COVID-19. *Journal of Mass Spectrometry and Advances in the Clinical lab* **2021**, *21*, 31–41.
- (16) Iles, R. K.; Zmuidinaite, R.; Iles, J. K.; Carnell, G.; Sampson, A.; Heeney, J. L. Development of a clinical MALDI-ToF mass spectrometry assay for SARS-CoV-2: rational design and multi-disciplinary team work. *Diagnostics* **2020**, *10*, 746.
- (17) Yoshinari, T.; Hayashi, K.; Hirose, S.; Ohya, K.; Ohnishi, T.; Watanabe, M.; Taharaguchi, S.; Mekata, H.; Taniguchi, T.; Maeda, T.; Orihara, Y.; Kawamura, R.; Arai, S.; Saito, Y.; Goda, Y.; Hara-Kudo, Y. Matrix-Assisted Laser Desorption and Ionization Time-of-Flight Mass Spectrometry Analysis for the Direct Detection of SARS-CoV-2 in Nasopharyngeal Swabs. *Anal. Chem.* **2022**, *94*, 4218–4226.
- (18) Swatkoski, S.; Russell, S.; Edwards, N.; Fenselau, C. Analysis of a model virus using residue-specific chemical cleavage and MALDI-TOF mass spectrometry. *Analytical chemistry* **2007**, *79*, 654–658.
- (19) Fenselau, C.; Demirev, P. A. Characterization of intact microorganisms by MALDI mass spectrometry. *Mass Spectrom. Rev.* **2001**, *20*, 157–171.
- (20) Fenselau, C.; Laine, O.; Swatkoski, S. Microwave assisted acid cleavage for denaturation and proteolysis of intact human adenovirus. *International journal of mass spectrometry* **2011**, *301*, 7–11.
- (21) Fenselau, C.; Laine, O.; Swatkoski, S. Microwave assisted acid cleavage for denaturation and proteolysis of intact human adenovirus. *International journal of mass spectrometry* **2011**, *301*, 7–11.
- (22) Turiello, R.; Dignan, L. M.; Thompson, B.; Poulter, M.; Hickey, J.; Chapman, J.; Landers, J. P. 2022. Centrifugal Microfluidic Method for Enrichment and Enzymatic Extraction of Severe Acute Respiratory Syndrome Coronavirus 2 RNA. *Analytical chemistry* **2022**, *94*, 3287–3295.
- (23) Clausen, T. M.; Sandoval, D. R.; Spliid, C. B.; Pihl, J.; Perrett, H. R.; Painter, C. D.; Narayanan, A.; Majowicz, S. A.; Kwong, E. M.; McVicar, R. N.; Thacker, B. E.; et al. SARS-CoV-2 infection depends on cellular heparan sulfate and ACE2. *Cell* **2020**, *183*, 1043–1057.
- (24) Hoffmann, D.; Mereiter, S.; Jin Oh, Y.; Monteil, V.; Elder, E.; Zhu, R.; Canena, D.; Hain, L.; Laurent, E.; Grünwald-Gruber, C.; Klausberger, M.; et al. Identification of lectin receptors for conserved SARS-CoV-2 glycosylation sites. *EMBO J.* **2021**, *40*, e108375.
- (25) Chen, D.; Bryden, W. A.; McLoughlin, M. A novel system for the comprehensive collection of nonvolatile molecules from human exhaled breath. *Journal of Breath Research* **2021**, *15*, 016001.
- (26) Chen, D.; Bryden, W. A.; Fenselau, C. Rapid analysis of ricin using hot acid digestion and MALDI-TOF mass spectrometry. *Journal of Mass Spectrometry* **2018**, *53*, 1013–1017.
- (27) Chen, D.; Bryden, W. A.; Fenselau, C. Microwave supported hydrolysis prepares *Bacillus* spores for proteomic analysis. *International journal of mass spectrometry* **2019**, *435*, 227–233.

(28) Gouveia, D.; Miotello, G.; Gallais, F.; Gaillard, J. C.; Debroas, S.; Bellanger, L.; Lavigne, J. P.; Sotto, A.; Grenga, L.; Pible, O.; Armengaud, J. Proteotyping SARS-CoV-2 virus from nasopharyngeal swabs: a proof-of-concept focused on a 3 min mass spectrometry window. *J. Proteome Res.* **2020**, *19*, 4407–4416.

(29) Nikolaev, E. N.; Indeykina, M. I.; Brzhozovskiy, A. G.; Bugrova, A. E.; Kononikhin, A. S.; Starodubtseva, N. L.; Petrotchenko, E. V.; Kovalev, G. I.; Borchers, C. H.; Sukhikh, G. T. Mass-spectrometric detection of SARS-CoV-2 virus in scrapings of the epithelium of the nasopharynx of infected patients via nucleocapsid N protein. *J. Proteome Res.* **2020**, *19*, 4393–4397.

(30) Ihling, C.; Tanzler, D.; Hagemann, S.; Kehlen, A.; Huttelmaier, S.; Arlt, C.; Sinz, A. Mass spectrometric identification of SARS-CoV-2 proteins from gargle solution samples of COVID-19 patients. *J. Proteome Res.* **2020**, *19*, 4389–4392.

(31) Bezstarosti, K.; Lamers, M. M.; Doff, W. A.; Wever, P. C.; Thai, K. T.; van Kampen, J. J.; Haagmans, B. L.; Demmers, J. A. Targeted proteomics as a tool to detect SARS-CoV-2 proteins in clinical specimens. *PLoS one* **2021**, *16*, e0259165.

(32) Saadi, J.; Oueslati, S.; Bellanger, L.; Gallais, F.; Dortet, L.; Roque-Afonso, A. M.; Junot, C.; Naas, T.; Fenaille, F.; Becher, F. Quantitative assessment of SARS-CoV-2 virus in nasopharyngeal swabs stored in transport medium by a straightforward LC-MS/MS assay targeting nucleocapsid, membrane, and spike proteins. *J. Proteome Res.* **2021**, *20*, 1434–1443.

(33) Shefcheck, K.; Yao, X.; Fenselau, C. Fractionation of cytosolic proteins on an immobilized heparin column. *Analytical chemistry* **2003**, *75*, 1691–1698.

(34) Bundy, J.; Fenselau, C. Lectin-based affinity capture for MALDI-MS analysis of bacteria. *Analytical chemistry* **1999**, *71*, 1460–1463.

(35) Bundy, J. L.; Fenselau, C. Lectin and carbohydrate affinity capture surfaces for mass spectrometric analysis of microorganisms. *Analytical chemistry* **2001**, *73*, 751–757.

(36) Hoyt, K.; Barr, J. R.; Kalb, S. R. Detection of ricin activity and structure by using novel galactose-terminated magnetic bead extraction coupled with mass spectrometric detection. *Anal. Biochem.* **2021**, *631*, 114364.

(37) Peccia, J.; Zulli, A.; Brackney, D. E.; Grubaugh, N. D.; Kaplan, E. H.; Casanovas-Massana, A.; Ko, A. I.; Malik, A. A.; Wang, D.; Wang, M.; Warren, J. L.; Weinberger, D. M.; Arnold, W.; Omer, S. B. Measurement of SARS-CoV-2 RNA in wastewater tracks community infection dynamics. *Nat. Biotechnol.* **2020**, *38*, 1164–1167.

(38) Cagno, V.; Tseligka, E. D.; Jones, S. T.; Tapparel, C. Heparan sulfate proteoglycans and viral attachment: true receptors or adaptation bias? *Viruses* **2019**, *11*, 596.

(39) Koehler, M.; Delguste, M.; Sieben, C.; Gillet, L.; Alsteens, D. Initial step of virus entry: virion binding to cell-surface glycans. *Annual review of virology* **2020**, *7*, 143–165.

(40) Stencel-Baerenwald, J. E.; Reiss, K.; Reiter, D. M.; Stehle, T.; Dermody, T. S. The sweet spot: defining virus–sialic acid interactions. *Nature Reviews Microbiology* **2014**, *12*, 739–749.

(41) Milewska, A.; Zarebski, M.; Nowak, P.; Stozek, K.; Potempa, J.; Pirc, K. Human coronavirus NL63 utilizes heparan sulfate proteoglycans for attachment to target cells. *Journal of virology* **2014**, *88*, 13221–13230.

(42) Ozaras, R.; Cirpin, R.; Duran, A.; Duman, H.; Arslan, O.; Bakan, Y.; Kaya, M.; Mutlu, H.; Isayeva, L.; Kebanlı, F.; Deger, B. A.; Bekeshev, E.; Kaya, F.; Bilir, S. Influenza and COVID-19 coinfection: report of six cases and review of the literature. *J. Med. Virol.* **2020**, *92*, 2657–2665.